Spectral Characteristics of Random Carrier Frequency Switching in Off-Line Switched Mode Power Supply

K. K. Tse, *Student Member, IEEE*, Henry S. H. Chung, *Member, IEEE*,
S. Y. R. Hui, *Senior Member, IEEE*, and H. C. So, *Member, IEEE*

Department of Electronic Engineering
City University of Hong Kong
Tat Chee Avenue
Kowloon Tong, Kowloon, Hong Kong.

Abstract – **In this paper, a detailed analysis and the spectral characteristics of a random carrier-frequency (RCF) technique for suppressing conducted EMI in an off-line switched-mode power supply are presented. The analysis provides a theoretical platform for studying the characteristics of this random switching scheme. The level of randomness is defined for the RCF scheme and varied in the converter example so that its effects on the power spectra can be demonstrated. Theoretical predictions of the spectral characteristics of this scheme are confirmed with measurements. Comparisons of the spectral performance show that the RCF scheme has better conducted EMI suppression than the FM and standard PWM schemes.**

I. Introduction

Nowadays, switched-mode power supplies have to be designed not only to provide the required electrical functions, but also to meet international electromagnetic compatibility (EMC) standards. Recently, random switching technique has been recognized as an emerging technology for power converters [3]. Various random switching schemes, which are originated from statistical communication theory [11], have been reported for dc/ac and dc/dc power conversion [3]-[10]. The basic principle of introducing randomness into standard PWM scheme is to spread out the harmonic power so that no harmonic of significant magnitude exists. This can be an effective way of suppressing EMI emission.

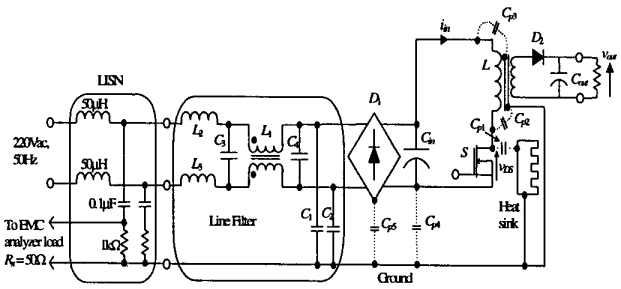

Fig. 1. Typical configuration of an off-line switched-mode power supply with conducted EMI test setup.

In [10], the cause of low-frequency noise on the dc/dc converter's output has been highlighted in the random pulse width modulation (RPWM) and random pulse position modulation (RPPM) schemes. Rigorous analyses of these two random schemes for DC-DC converters have been presented in [12, 13].

In this paper, the random carrier frequency (RCF) scheme for DC-DC converter is examined and compared with the standard PWM scheme and the FM [2] scheme. One attractive feature of the RCF scheme is that it inherently ensures constant duty cycle operation in DC-DC converter. The variation of the output voltage is not as significant as the RPWM and RPPM schemes and therefore allows simple feedback control design. The suppression of EMI emission has been verified experimentally in [7]-[9]. However, the lack of theory of such scheme makes it difficult to decide how much randomness should be introduced. This paper shows a mathematical analysis of the above phenomena of the RCF method. It aims at providing a platform for understanding the spectral performance and the effect of the variation of the level of randomness. The model of an off-line switched-mode power supply and mathematical derivations of the frequency spectra of the input current and the switch voltage waveform with and without RCF scheme are presented in Section II. Practical measurements of the conducted EMI of a 100W, 220V/24V, 50Hz off-line flyback converter are given in Section III, together with analytical predictions. The results are compared with the standard constant switching frequency scheme and the FM [2] scheme. The conclusion follows in Section IV.

II. Models And Mathematical Derivations

A. Source of EMI

A typical configuration with the conducted electromagnetic interference (EMI) test setup [1] is shown in Fig. 1, a standard line-impedance stabilization network (LISN) is connected between the power supply and the supply lines. As the supply source impedance is high, a common-mode harmonic current i_h, from the switch voltage, will flow through the ground plane, parasitic capacitance $C_{p1} \sim C_{p5}$, C_1,

0-7803-5160-6/99/$10.00 © 1999 IEEE.

and C_2. If C_p denotes the effective parasitic capacitance between the drain voltage of the switch S (i.e., v_S) and the ground plane, the spectral magnitude of i_h at frequency f, $|I_h(f)|$, can be obtained by

$$|I_h(f)| = |V_S(f)|\, 2\pi f C_p \,. \tag{1}$$

where $|V_S(f)|$ is the spectral magnitude of v_S. Thus, the spectral magnitude of the voltage across C_1 and C_2, $|V_h(f)|$, can be approximated by

$$|V_h(f)| = |I_h(f)| X_C = \frac{|I_h(f)|}{2\pi f C} \tag{2}$$

if $C_1 = C_2 = C$.

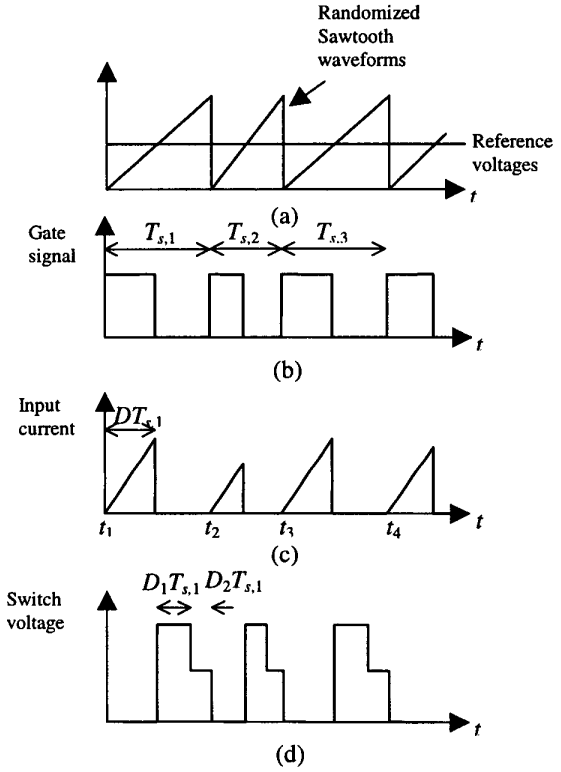

Fig. 2. Waveforms of flyback converter operating in discontinuous conduction mode with RCF scheme. (a) Sawtooth and reference voltage waveforms. (b) Gate signal. (c) Input current. (d) Switch voltage.

For the input side, since L_1, L_2, and L_3 form a potential divider with the simulated 50Ω supply line resistance R_x in the LISN, part of v_h appears on R_x. Thus, in order to reduce the voltage across R_x, L_1, L_2, and L_3 can be increased. However, this will substantially decrease the voltage supplying to the converter circuit, due to the increase in the voltage drop across L_1, L_2, and L_3.

In this study, the RCF scheme is applied to the PWM switching of the main switch S. Fig. 2(a) shows the randomized sawtooth waveform that is compared with a reference signal to generate the gate signal [Fig. 2(b)]. The duty cycle D of S is fixed in the respective cycle, although the switching period (stochastic variable) T_s is varied. Spreading the harmonic power of the input current and the switch voltage signal is discussed separately in the following sub-sections. The mathematical derivations are based on a flyback converter operating in discontinuous conduction mode (DCM), which is a commonly used configuration in many low-power applications.

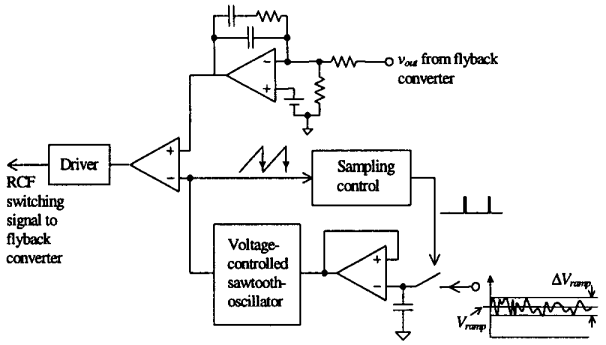

Fig. 3. Synthesis of RCF switching signal.

B. Spectral Characteristics of the Input Current Waveform

Fig. 2(c) shows the waveform of the input current i_{in} of the converter. For a generic switching cycle k, T_s equals $T_{s,k}$. $i_{in,k}(t)$ can be expressed as

$$i_{in,k}(t - t_k) = \begin{cases} \dfrac{V_{in}}{L} t & for \quad t_k \le t \le DT_{s,k} \\ 0 & \text{elsewhere.} \end{cases} \tag{3}$$

where V_{in} is the input voltage and L is the inductance of the flyback transformer. T_s is a randomized switching period resulting from the RCF. The general expression of $i_{in}(t)$ is

$$i_{in}(t) = \lim_{N \to \infty} \sum_{k=1}^{N} i_{in,k}(t - t_k) \,. \tag{4}$$

By using Wiener-Khintchine theorem, the power spectrum of $i_{in}(t)$ can be obtained by

$$S_{i_{in}}(f) = \lim_{T_O \to \infty} \frac{E[|I_{in,T_O}(f)|^2]}{T_O} \,, \tag{5}$$

where $E[\cdot]$ indicates the expected value and $I_{in,T_O}(f)$ is the Fourier transform of $i_{in}(t)$ over the time-record of T_O. By substituting (4) into (5), (5) can be implemented to be

$$S_{i_{in}}(f)=\lim_{N\to\infty}\frac{1}{N\,E[T_s]}\sum_{k=1}^{N}\sum_{l=1}^{N}E[I_{in,l}(f)\,I^{*}_{in,k}(f)e^{j2\pi f(t_k-t_l)}] \tag{5}$$

where $I_{in,l}(f)$ and $I_{in,k}(f)$ are the Fourier transform of $i_{in,l}(t)$ and $i_{in,k}(t)$, respectively. To follow the methodology in [11], (5) is substantially simplified as the follow:

$$S_{i_{in}}(f)=\frac{1}{E[T_s]}\{E[|I_{in}(f)|^2] + 2\mathrm{Re}\{\frac{E[I_{in}(f)e^{j2\pi fT_s}]E[I^{*}_{in}(f)]}{1-E[e^{j2\pi fT_s}]}\}\} \tag{6}$$

This is a general expression for RCF switching schemes under consideration if $I_{in}(f)$ is substituted by the Fourier transform of a cycle of the considered signal. In Section II-C, the derivation of power spectrum of switch voltage is based on (15).

i) Standard Constant Switching Frequency (standard) Scheme

If the converter operates with standard scheme, (14) is modified with

$$I_{in,l}(f)=I_{in,k}(f)=I_{in}(f); \tag{7}$$

$$t_{k+1}-t_k=T_s; \tag{8}$$

and the Poisson identity,

$$\sum_{k=1}^{\infty}e^{j2\pi kfT_s}=f_s\sum_{k=1}^{\infty}\delta(f-kf_s) \tag{9}$$

where T_s is a constant, $f_s=\frac{1}{T_s}$. Thus, the power spectrum of i_{in} in the standard scheme is

$$S_{i_{in}}(f)=\frac{1}{T_s^{\,2}}|I_{in}(f)|^2\sum_{k=1}^{\infty}\delta(f-kf_s)\ . \tag{10}$$

By (3), the Fourier transform of a cycle of i_{in} is

$$I_{in}(f)=\int_0^{DT_s}\frac{V_{in}}{L}te^{-j2\pi ft}\,dt =\frac{V_{in}}{j2\pi fL}e^{-j\pi fDT_s}[\frac{\sin(\pi fDT_s)}{\pi f}-DT_s\,e^{-j\pi fDT_s}]. \tag{11}$$

Thus, the squared absolute value is

$$|I_{in}(f)|^2=\frac{2V_{in}^{\,2}}{(2\pi f)^4L^2}[1-\cos(2\pi fDT_s)-2\pi fDT_s\sin(2\pi fDT_s)+\frac{(2\pi fDT_s)^2}{2}]. \tag{12}$$

For the standard scheme, $S_{i_{in}}(f)$ is determined by substituting (12) into (10).

ii) RCF Scheme

Assume that the randomness of T_s is subject to a probability density function $P(T_s)$, which has the uniform distribution with upper limit T_2 and lower limit T_1 (i.e., $T_s\in[T_1,T_2]$). Let ΔT_s denote the period deviation and $\Re$ denote the level of randomness on T_k,

$$\Delta T_s=T_2-T_1 \tag{13}$$

$$\Re=\frac{\Delta T_s}{E[T_s]}. \tag{14}$$

Hence, the probability density function of T_s is of the form

$$P(T_s)=\begin{cases}\frac{1}{\Delta T_s}=\frac{1}{\Re E[T_s]}, & T_1\le T_s\le T_2\\ 0 & \text{Otherwise.}\end{cases} \tag{15}$$

$$E[|I_{in}(f)|^2]=\frac{2V_{in}^{\,2}}{(2\pi f)^4L^2\Re E[T_s]}\times\{\Re E[T_s]-\frac{1}{\pi fD}[\sin(2\pi fDT_2)-\sin(2\pi fDT_1)]+T_2\cos(2\pi fDT_2)-T_1\cos(2\pi fDT_1)+\frac{(2\pi fD)^2}{6}(T_2^{\,3}-T_1^{\,3})\}, \tag{16}$$

$$E[I_{in}(f)e^{j2\pi fT_s}]=\frac{V_{in}}{j(2\pi f)^3L\Re E[T_s]}\times\{\{\frac{1}{1-D}-\frac{D[1-j2\pi f(1-D)T_2]}{(1-D)^2}\}e^{j2\pi f(1-D)T_2}-\{\frac{1}{1-D}-\frac{D[1-j2\pi f(1-D)T_1]}{(1-D)^2}\}e^{j2\pi f(1-D)T_1}-e^{j2\pi fT_2}+e^{j2\pi fT_1}\}, \tag{17}$$

$$E[I^{*}_{in}(f)]=\frac{V_{in}}{j(2\pi f)^3LD\Re E[T_s]}\times\{(2-j2\pi fDT_2)e^{j2\pi fDT_2}-(2-j2\pi fDT_1)e^{j2\pi fDT_1}-j2\pi fD\Re E[T_s]\}. \tag{18}$$

By substituting (14)-(18) into (6), $S_{i_{in}}(f)$ in the RCF scheme can be found. As will be shown in Section III, $S_{i_{in}}(f)$ will become close to a continuous spectrum as $\Re$ increases.

C. Spectral Characteristics of the Switch Voltage Waveform

The waveform of the drain-source voltage v_{DS} of S in Fig. 2(d) is expressed as

$$v_{DS}(t)=\begin{cases}0 & for \quad 0\le t\le DT_k\\ V_{in}+n\,v_{out}=V_M & for \quad DT_k<t\le D_1T_k\\ V_{in} & for \quad D_1T_k<t\le T_k\end{cases} \tag{19}$$

where n is the turns ratio of the flyback transformer and v_{out} is the output voltage, which is equal to

$$v_{out}=\sqrt{\frac{RT_s}{2L}}\,DV_{in} \tag{20}$$

where R is the output load resistance.

$$D_1=\frac{DV_{in}}{n\,v_{out}}; \tag{21}$$

$$D_2=1-D-D_1. \tag{22}$$

Following the similar approach for i_{in}, the power spectrum $S_{v_{DS}}(f)$ can be expressed as,

$$S_{v_{DS}}(f)=\frac{1}{E[T_s]}\{E[|V_{DS}(f)|^2]+2\mathrm{Re}\{\frac{E[V_{DS}(f)e^{j2\pi fT_s}]\,E[V_{DS}^*(f)]}{1-E[e^{j2\pi fT_s}]}\}\} \quad \text{for } f\neq 0. \tag{23}$$

i) Standard Constant Switching Frequency (Standard) scheme

For the standard scheme, T_s is a constant and

$$S_{v_{DS}}(f)=\frac{1}{T_s^2}|V_{DS}(f)|^2\sum_{k=1}^{\infty}\delta(f-k\,f_s). \tag{24}$$

The Fourier transform of a cycle of v_{DS} is

$$\begin{aligned}V_{DS}(f)&=\int_0^T v_{DS}(t)\,e^{-j2\pi ft}dt\\ &=V_M\,\frac{\sin(\pi f\,D_1T_s)}{\pi f}e^{-j\pi f\,D_1T_s}\,e^{-j2\pi f\,DT_s}+\\ &\quad V_{in}\,\frac{\sin(\pi f\,D_2T_s)}{\pi f}e^{-j\pi f\,D_2T_s}\,e^{-j2\pi f(1-D_2)T_s}\end{aligned} \tag{25}$$

and hence, its squared absolute value is given as

$$\begin{aligned}|V_{DS}(f)|^2=\frac{2}{(2\pi f)^2}\{&V_M^2+V_{in}^2-V_M\,V_{in}-\\ &V_M\,V_{in}\cos[2\pi f(1-D)\,T_s]-\\ &(V_M^2-V_M\,V_{in})\cos(2\pi f\,D_1T_s)-\\ &(V_{in}^2-V_M\,V_{in})\cos(2\pi f\,D_2T_s)\}.\end{aligned} \tag{26}$$

ii) RCF Scheme

In order to calculate $S_{v_{DS}}(f)$, (24) is used. With the same assumptions of randomness of T_s in (15), the expected values of the terms in (34) can be expressed as follows,

$$\begin{aligned}&E\{|V_{DS}(f)|^2\}\\ &=\frac{2}{(2\pi f)^3\,\Re E[T_s]}\{(V_M^2+V_{in}^2-V_MV_{in})(2\pi f)\Re E[T_s]-\\ &\frac{V_M\,V_{in}}{1-D}\{\sin[2\pi f(1-D)T_2]-\sin[2\pi f(1-D)T_1]\}-\\ &\frac{(V_M^2-V_M\,V_{in})}{D_1}[\sin(2\pi f\,D_1T_2)-\sin(2\pi f\,D_1T_1)]-\\ &\frac{V_{in}^2-V_M\,V_{in}}{D_2}[\sin(2\pi f\,D_2T_2)-\sin(2\pi f\,D_2T_1)]\},\end{aligned} \tag{27}$$

$$\begin{aligned}&E[V_{DS}(f)e^{j2\pi fT_s}]\\ &=\frac{1}{(2\pi f)^2\,\Re E[T_s]}\{j(2\pi f)\,\Re E[T_s]V_{in}-\\ &\frac{V_M}{1-D}[e^{j2\pi f(1-D)T_2}-e^{j2\pi f(1-D)T_1}]+\\ &\frac{V_M-V_{in}}{D_2}(e^{j2\pi f\,D_2T_2}-e^{j2\pi f\,D_2T_1}),\end{aligned} \tag{28}$$

$$\begin{aligned}&E[V_{DS}^*(f)]\\ &=\frac{1}{(2\pi f)^2\,\Re E[T_s]}\times\\ &[\frac{V_M}{D}(e^{j2\pi f\,DT_2}-e^{j2\pi f\,DT_1})+\\ &\frac{V_{in}-V_M}{D+D_2}(e^{j2\pi f(1-D_2)T_2}-e^{j2\pi f(1-D_2)T_1})-\\ &V_{in}(e^{j2\pi fT_2}-e^{j2\pi fT_1})].\end{aligned} \tag{29}$$

Similar to the characteristics of the input current $S_{v_{DS}}(f)$ will be changed from a discrete harmonic spectrum to a continuous spectrum as the level of randomness in T_s increases.

III. Experimental Verifications

Fig. 3 shows the synthesis of RCF switching signal for the off-line flyback converter shown in Fig. 1. The component values of the converter are tabulated in Table I. A composite random signal, which contains a fixed dc signal V_{ramp} and a noise with maximum amplitude ΔV_{ramp}, generates the randomized sawtooth signal. The level of randomness $\Re$ in the RCF scheme can also be defined as

$$\Re = \frac{\Delta V_{ramp}}{V_{ramp}} \tag{30}$$

At the end of every switching cycle, the composite random signal is sampled and then fed to a voltage controlled oscillator (VCO) to generate the next sawtooth cycle. The nominal switching frequency is set at 50kHz. $\Re = 0$ corresponds to the standard PWM scheme and the switching frequency is 50kHz. When $\Re = 0.2$, the switching frequency is uniformly randomized within the frequency range from 45kHz to 55kHz. Fig. 4 shows the experimental voltage and current waveforms of the converter's main switch when $\Re = 0$ and $\Re = 0.2$, respectively. The output voltage

Table I Component values of a practical off-line flyback converter.

Converter	Line Filter
L = 1mH	L_1 = 0.93mH
C_{in} = 220μF	$L_2 = L_3$ =1mH
C_{out} = 470μF	$C_1 = C_2$ = 3.3nF
D_1 = 1N4004s	$C_3 = C_4$ = 0.1μF
D_2 = MUR460	
S = IRF840	
Turn ratio = 5	

under two cases is maintained at 24V with ripple voltage of about 400mV. Experimental measurements of the power spectra of i_{in} [i.e., $S_{\exp,i_{in}}(f)$] and v_{DS} [i.e., $S_{\exp,v_{DS}}(f)$] are shown in Fig. 5. The results were taken from a signal analyzer HP89410A with the use of the Hanning window, 4096 time samples, and a sampling rate of 2.5MHz.

It is important to note that the true power spectrum derived in Section II is based on infinite time-records of the RCF switching signal. However, as pointed out in [14], power spectra obtained from digital signal processing technique are strictly speaking approximations because of the

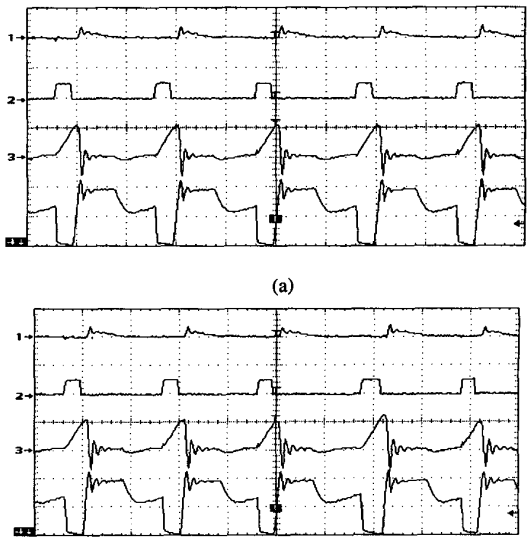

(a)

(b)

Fig. 4 Experimental waveforms of the converter. (a) $\Re = 0$. (b) $\Re = 0.2$. Channel 1: Output voltage (1V/div, with ac couple). Channel 2: Gate signal (10V/div). Channel 3: Input current (1A/div). Channel 4: Switch voltage (200V/div). Time : 10μs/div.

finite number of time records involved in the calculation. In order to make a better comparison of the theoretical power spectrum $S(f)$ and the experimental ones $S_{\exp}(f)$, a mathematical compensation for the analytical power spectrum $S'(f)$ is performed by convoluting $S(f)$ with the window function W. That is,

$$\begin{aligned} S'(f) &= S(f_0) * |W(f_0)|^2 \\ &= \frac{1}{2\pi}\int_{-\infty}^{\infty} S(f)\,|W(f-f_0)|^2\,df \end{aligned} \tag{31}$$

where f_0 is one of discrete frequency points given by FFT analysis, and the characteristic of the window function W is subject to the following factor in FFT-based processing:

(a) the type of windowing function,
(b) the number of sampled time-record, and
(c) the sampling rate.

By considering the above factors, the modified analytical solution $S'(f)$ is compared to the experimental $S_{\exp}(f)$ from the FFT-based spectrum analyzer, using the same parameters as HP89410A.

The analytical prediction of $S_{i_{in}}(f)$ and $S_{v_{DS}}(f)$ with $\Re = 0.2$ are shown in Fig. 6. They are determined by using (6) and (23), together with the treatment of (31). Both analytical and experimental results are in close agreement. It can be observed that the RCF technique substantially reduces the discrete switching frequency harmonics. The peak

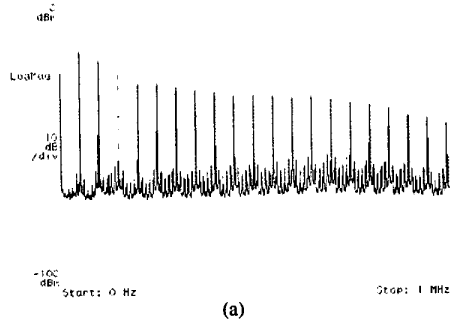

(a)

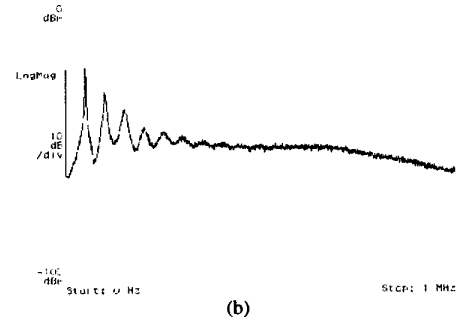

(b)

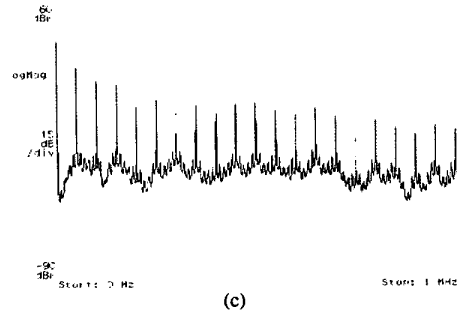

(c)

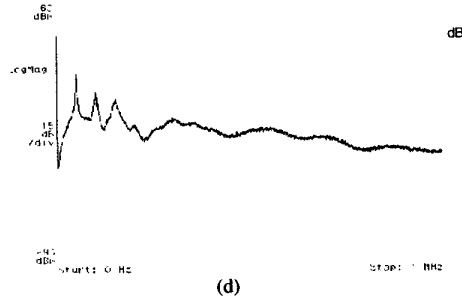

(d)

Fig. 5. Experimental power spectrum. (a) Input current with $\Re = 0$. (b) Input current with $\Re = 0.2$. (c) Switch voltage with $\Re = 0$. (d) Switch voltage with $\Re = 0.2$.

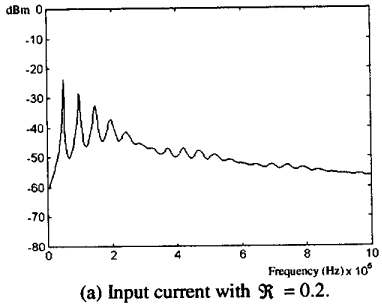

(a) Input current with $\Re = 0.2$.

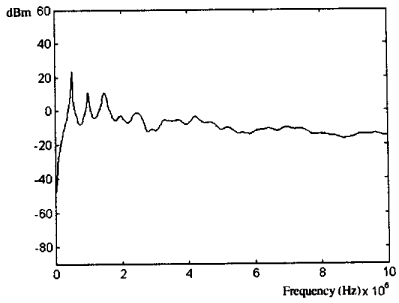

(b) Switch voltage with $\Re = 0.2$.

Fig. 6. Theoretical predictions of power spectra.

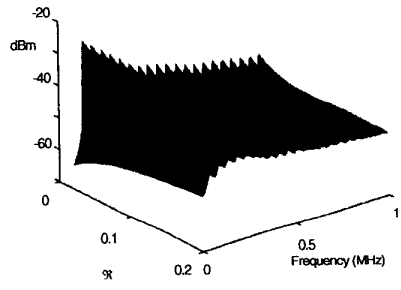

(a)

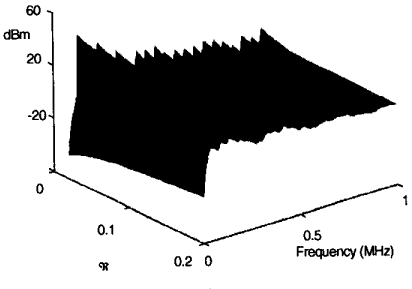

(b)

Fig. 7. Variations of the power spectrum with respect to the value of $\Re$. (a) Input current. (b) Switch voltage.

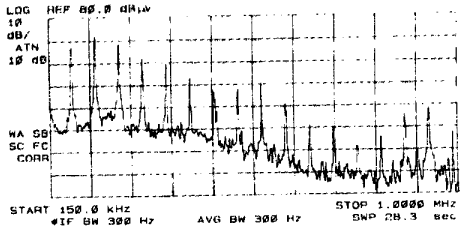

(a)

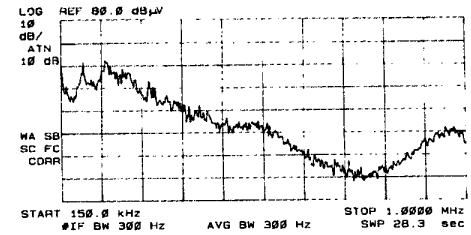

(b)

Fig. 8. Measured conducted emission. (a) $\Re = 0$. (b) $\Re = 0.2$.

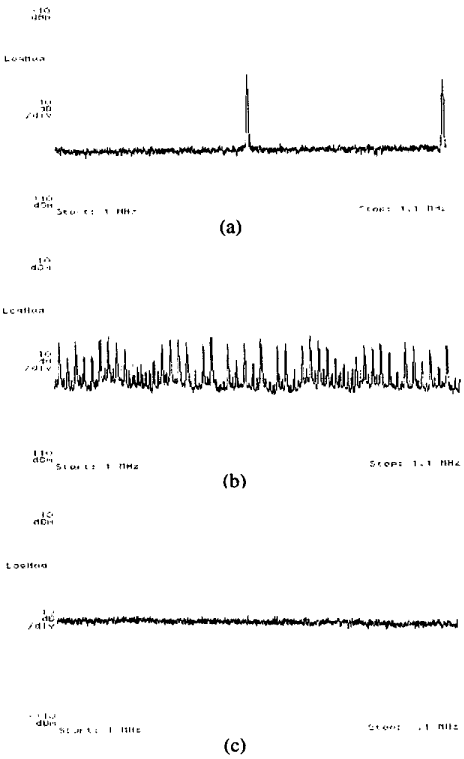

(a)

(b)

(c)

Fig. 9. Power spectrum of input current under (a) standard FSF scheme, (b) FM with 2KHz modulating signal, and (c) proposed RCF scheme.

harmonic power of the RCF scheme is much lower than that of the standard scheme. Using the theory developed, the variations of the power spectrum with respect to the value of $\Re$ are generated and shown in Fig.7. It is important to note that the power spectrum changes gradually from discrete harmonics spectrum to continuous noise spectrum with an increasing $\Re$. The overall envelope of the power spectrum also decreases as $\Re$ increases.

For the measurement of the conducted EMI of the converter, a LISN Farnell LSN30 and an EMC analyzer HP8591EM are used. Quasi-peak detector is used for all the testing. Fig. 8 shows the measured conducted emission under the above two cases. When $\Re = 0$, some discrete harmonics exist. With $\Re = 0.2$, the harmonics are spread over, demonstrating the effectiveness of using RCF in suppression of EMI of the off-line switched-mode power supply.

The RCF scheme is also compared with the FM scheme. Like the RCF scheme, the switching frequency of the FM scheme is allowed to vary within the frequency range from 45kHz to 55kHz. The FM scheme is modulated at 2kHz. Fig. 9 shows a comparison of the conducted EMI when the converter is operated with (i) the standard PWM [Fig. 9(a)], (ii) the FM of 2kHz on standard PWM [2] [Fig. 9(b)], and (iii) the RCF scheme [Fig. 9(c)]. It can be seen that the FM scheme manages to reduce the discrete harmonic components to some extent when compared with the standard PWM scheme. However, the RCF scheme offers the best conducted EMI suppression among the three schemes under consideration.

IV. Conclusions

An analysis on the random carrier frequency PWM method has been presented. The theory provides a mathematical platform for studying the spectral characteristic of this random PWM scheme. It has the effect of reducing conducted EMI emissions as demonstrated in an experimental prototype. Analytical prediction is verified with the practical measurements. The implementation here is simple and only involves a slight modification on existing circuits using standard PWM technique. In terms of conducted EMI suppression, this study also demonstrates that the RCF scheme is better than the FM scheme which has been incorporated into the PWM scheme of many commercial power converters.

References

[1] K. H. Billings, *Switchmode Power Supply Handbook*, McGraw Hill, 1989.

[2] F. Lin and D. Y. Chen, "Reduction of power supply EMI emission by switching frequency modulation," *IEEE Power Electronics Specialists Conference*, 1993, pp. 127-133.

[3] M. P. Kazmierkowski and F. Blaabjerb, "Impact of emerging technologies on PWM control of power electronic converters," *IEEE Industrial Electronics Society Newsletter*, December 1995, pp. 9-13.

[4] A. M. Stankovic, G. C. Verghese, and D. J. Perreault, "Analysis and synthesis of randomised modulation schemes for power converters," *IEEE Trans. Power Electron.*, vol. 10, no. 6, pp. 680-693, 1995.

[5] S. Y. R. Hui, I. Oppermann, and S. Sathiakumar, "Microprocessor based random PWM schemes for DC-AC power conversion," *IEEE Trans. Power Electron.*, vol. 12, no. 2, pp. 253-260, 1997.

[6] T. Tanaka, T. Ninomiya, and K. Harada, "Random switching control in dc-dc converters," *Proc. IEEE Power Electronics Specialists Conference*, 1989, pp. 500-507.

[7] D. S. Stone and B. Chambers, "The effect of carrier frequency modulation of PWM waveforms on conducted EMC problems in Switched Mode Power Supplies," *EPE Journals*, vol. 5, no.3, pp. 32-37, Jan. 1996.

[8] D. A. Stone and B. Chambers, "Effect of spread-spectrum modulation of switched mode power converter PWM carrier frequencies on conducted EMI," *Electronics Letters*, vol. 31, no. 10, pp. 769-770, May 1995.

[9] D. A. Stone and B. Chambers, "Easing problems in switched mode power converters by random modulation of the PWM carrier frequency," in *Proc. Applied Power Electronics Specialists Conference*, 1996, pp. 327-332.

[10] Y. Shrivastava, S. Y. R. Hui, S. Sathiakumar, H. Chung and K. K. Tse, "Effects of continuous noise in randomised switching DC-DC converters," *Electronics Letters*, vol. 33, no. 11, pp. 919-921, May 1997.

[11] D. Middleton, *An Introduction to Statistical Communication Theory*, McGraw-Hill Book Company Inc.

[12] Y. Shrivastava, S. Y. R. Hui, S. Sathiakumar, H. Chung and K. K. Tse, "Harmonic analysis of non-deterministic switching methods for dc-dc power converters," *IEEE Trans. Circuits Systs. – Part I.* (Accepted for publication)

[13] Y. Shrivastava, S. Y. R. Hui, S. Sathiakumar, H. Chung and K. K. Tse, "A comparison of deterministic and non-deterministic switching methods for dc-dc converters," *IEEE Trans. Power Electron.* (Accepted for publication)

[14] M. M. Bech, J. K. Pedersen, F. Blaabjerg, and A. M. Trzynadlowski, "A methodology for true comparison of analytical and measured frequency domain spectra in random PWM converters," in *Proc. IEEE Power Electronics Specialists Conference*, 1998, pp. 36-43.